Remote Sensing of Environment 114 (2010) 1178–1189

Contents lists available at ScienceDirect

Remote Sensing of Environment

journal homepage: www.elsevier.com/locate/rse

Estimating northern peatland CO_2 exchange from MODIS time series data

Per Schubert [a,*], Lars Eklundh [a], Magnus Lund [a], Mats Nilsson [b]

[a] Department of Earth and Ecosystem Sciences, Faculty of Science, Lund University, Sölvegatan 12, SE-223 62 Lund, Sweden
[b] Department of Forest Ecology and Management, Faculty of Forest Sciences, Swedish University of Agricultural Sciences, Skogsmarksgränd, SE-901 83 Umeå, Sweden

ARTICLE INFO

Article history:
Received 28 August 2009
Received in revised form 7 January 2010
Accepted 9 January 2010

Keywords:
Ecosystem respiration (ER)
Enhanced vegetation index (EVI)
Gross primary productivity (GPP)
Land surface temperature (LST)
Moderate Resolution Imaging Spectroradiometer (MODIS)
Net ecosystem exchange (NEE)
Peatland
Photosynthetic photon flux density (PPFD)

ABSTRACT

Studies using satellite sensor-derived data as input to models for CO_2 exchange show promising results for closed forest stands. There is a need for extending this approach to other land cover types, in order to carry out large-scale monitoring of CO_2 exchange. In this study, three years of eddy covariance data from two peatlands in Sweden were averaged for 16-day composite periods and related to data from the Moderate Resolution Imaging Spectroradiometer (MODIS) and modeled photosynthetic photon flux density (PPFD). Noise in the time series of MODIS 250 m vegetation indices was reduced by using double logistic curve fits. Smoothed normalized difference vegetation index (NDVI) showed saturation during summertime, and the enhanced vegetation index (EVI) generally gave better results in explaining gross primary productivity (GPP). The strong linear relationships found between GPP and the product of EVI and modeled PPFD ($R^2 = 0.85$ and 0.76) were only slightly stronger than for the product of EVI and MODIS daytime 1 km land surface temperature (LST) ($R^2 = 0.84$ and 0.71). One probable reason for these results is that several controls on GPP were related to both modeled PPFD and daytime LST. Since ecosystem respiration (ER) was largely explained by diurnal LST in exponential relationships ($R^2 = 0.89$ and 0.83), net ecosystem exchange (NEE) was directly related to diurnal LST in combination with the product of EVI and modeled PPFD in multiple exponential regressions ($R^2 = 0.81$ and 0.73). Even though the R^2 values were somewhat weaker for NEE, compared to GPP and ER, the RMSE values were much lower than if NEE would have been estimated as the sum of GPP and ER. The overall conclusion of this study is that regression models driven by satellite sensor-derived data and modeled PPFD can be used to estimate CO_2 fluxes in peatlands.

© 2010 Elsevier Inc. All rights reserved.

1. Introduction

Studies have shown that mid- to high-latitude forests at the Northern Hemisphere probably can explain the so-called "missing sink" for atmospheric carbon dioxide (CO_2) (Keeling et al., 1996; Prentice et al., 2001). Research has therefore focused on forest CO_2 exchange, with less attention given to other ecosystem types, until recently. Peatlands are important in the carbon cycle, since they may store 30% of the global soil carbon or 50% of the carbon currently in the atmosphere (Gorham, 1991; Turunen et al., 2002). The major fraction of all peatlands is located in northern temperate and cold climates (Aselmann & Crutzen, 1989). Because of waterlogged, anoxic, and cool conditions, peatlands are characterized by slow decomposition rates, which together with photosynthesis results in the accumulation of atmospheric CO_2. However, there are concerns that increased temperatures and evapotranspiration rates will cause drought conditions and a subsequent release of CO_2 (Gorham, 1991; Tarnocai, 2006; Aurela et al., 2007). In sub-arctic peatlands, temperature increases may lead to permafrost melting, affecting the physical stability of the ground and the biological dynamics of the soil and potentially having severe consequences for the carbon storage (Gorham, 1991; Johansson et al., 2006; Tarnocai, 2006). For these reasons, it is of particular interest to find suitable ways of extending estimates of CO_2 exchange in peatlands, across time and space.

An important method of measuring CO_2 exchange for extended time periods is the eddy covariance technique (Wofsy et al., 1993; Lindroth et al., 1998; Aubinet et al., 2000; Falge et al., 2001). In the mid- and high-latitudes, an increasing number of eddy covariance tower sites cover a variety of ecosystems, such as forests, grasslands, wetlands, and agricultural lands (Baldocchi et al., 2001; Baldocchi, 2003). Still, these on-site measurements are restricted in space, and therefore, do not represent the diversity of different species, age classes, and site conditions at a larger scale (Lagergren et al., 2006).

One way to extend estimates of CO_2 exchange to a larger spatial scale is to use satellite sensor-derived data as input to a light use efficiency (LUE, see Appendix for abbreviations and symbols) model, developed by e.g. Monteith (1972, 1977) and Prince (1991). It is well known that the LUE model comes in the two versions where either gross primary productivity (GPP) or net primary productivity (NPP) is expressed as the product of the photosynthetically active radiation absorbed by vegetation (APAR) and the light use efficiency factor (ε). While GPP is the total amount of CO_2 taken up by photosynthesis, NPP

* Corresponding author. Department of Earth and Ecosystem Sciences, Lund University, Sölvegatan 12, SE-223 62 Lund, Sweden. Tel.: +46 46 2223830; fax: +46 46 2224011.
E-mail address: per.schubert@nateko.lu.se (P. Schubert).

0034-4257/$ – see front matter © 2010 Elsevier Inc. All rights reserved.
doi:10.1016/j.rse.2010.01.005

is the CO_2 uptake after subtraction of autotrophic respiration, and ε is the vegetation capacity to convert radiation energy into biomass. It has been shown that the fraction of absorbed photosynthetically active radiation (FAPAR) is dependent on the normalized difference vegetation index (NDVI; Rouse et al., 1973) and that the relationship is linear (Asrar et al., 1984, 1992; Goward & Huemmrich, 1992; Myneni & Williams, 1994). Therefore, satellite sensor-derived NDVI has been used to derive FAPAR (Tucker et al., 1986; Chen, 1996; Fensholt et al., 2004; Olofsson & Eklundh, 2007), and when FAPAR is available, APAR is easily calculated by multiplying FAPAR with the incoming photosynthetically active radiation (PAR).

For Scandinavian coniferous forests, Olofsson et al. (2007) used NDVI from the Moderate Resolution Imaging Spectroradiometer (MODIS) to derive FAPAR, and then, calculated APAR by multiplying FAPAR with modeled PAR. The LUE model was used to estimate NPP, with ε dependent on latitude, air temperature (AT), and the day of the year (DOY) (Lagergren et al., 2005). For North European coniferous and deciduous forests, Olofsson et al. (2008) adopted another approach without any separate estimation of ε. Eddy covariance GPP was modeled with a regression function driven by APAR and the MODIS enhanced vegetation index (EVI; Huete et al., 2002). By reducing atmosphere and canopy background influences, EVI enhance the vegetation signal and maintains sensitivity in high biomass regions:

$$EVI = G\frac{\rho_{NIR}-\rho_{red}}{\rho_{NIR} + C_1\rho_{red} - C_2\rho_{blue} + L}, \quad (1)$$

where ρ_{NIR}, ρ_{red}, and ρ_{blue}, are surface reflectance values in the near infrared (NIR), red, and blue wavelength bands, respectively. The coefficients $C_1 = 6$ and $C_2 = 7.5$ correct for atmosphere influences, while $L = 1$ adjust for the canopy background. The factor $G = 2.5$ is the gain factor. To achieve APAR, Olofsson et al. (2008) derived FAPAR from NDVI and multiplied it with measured PAR. Furthermore, ecosystem respiration (ER) was modeled with a regression function driven by AT, and net ecosystem exchange (NEE) was finally calculated from GPP and ER. Both Olofsson et al. (2007) and Olofsson et al. (2008) used eddy covariance data to validate modeled CO_2 fluxes, and stronger relationships were obtained for GPP and ER, than for NEE.

For North American coniferous and deciduous forests, Rahman et al. (2005) found an equally strong relationship between eddy covariance GPP and MODIS EVI as for eddy covariance GPP and the MODIS GPP product (MOD17; Running et al., 2004). It was also found that nighttime ER was related to nighttime MODIS land surface temperature (LST). In a subsequent study with additional sites, Sims et al. (2006) found that EVI performed even better than MODIS GPP. This was later confirmed by Sims et al. (2008) and implemented in their temperature and greenness (TG) model, which improved the results by combining EVI and LST. Therefore, it was suggested that simpler models based entirely on satellite sensor-derived data could be as good as the MODIS GPP product.

Heinsch et al. (2006) evaluated the LUE-based 1 km MODIS GPP product (MOD17) and indicated that the input of coarse resolution meteorological data is the most limiting factor in the quality of the product. It was also pointed out that the 1 km land cover product (MOD12Q1), used in the MOD17 algorithm, has a too coarse resolution to be applied in regions with heterogeneous vegetation. An additional problem is that the particular land cover classification scheme in MOD12Q1 (the product contains multiple schemes) used to extract ε from lookup tables does not have any category for peatlands (Heinsch et al., 2003). In their study of peatland representation on global maps, Krankina et al. (2008) investigated the MOD12Q1 product based on another classification scheme that includes a category for peatlands. This scheme is used to derive FAPAR as input to the MOD17 algorithm. It was found that peatlands are highly underrepresented, compared to a detailed map of the St. Petersburg region in Russia. Since peatlands often are smaller areas located within a mosaic of other land cover types, such as temperate and boreal forests, it seems that the MOD17 product cannot account for the site-specific conditions in peatlands. Although these studies focused on 1 km MODIS products, it is reasonable to assume general resolution difficulties associated with peatlands.

An additional problem with peatlands is that investigations both in the laboratory and in the field have demonstrated that *Sphagnum* mosses, which dominate most peatland types, have distinctively different spectral signatures compared to vascular vegetation (Vogelmann & Moss, 1993; Hall et al., 1995; Bubier et al., 1997; Bryant & Baird, 2003). According to Bubier et al. (1997), the narrow red absorptions and near-infrared (NIR) peaks of *Sphagnum* mosses, which are dominant in this study, make NDVI and the simple vegetation index ratio inappropriate for characterizing biomass or greenness. Also, Vogelmann & Moss (1993) and Bubier et al. (1997) show that the differences between the red and NIR reflectance values are smaller for *Sphagnum* mosses, which generates lower NDVI values. For the seasonal variation in NDVI, this should mean that the errors in data are larger in relation to the range, making it harder to find strong relationships with other seasonal variables.

Evidently, there are problems to be solved, but satellite sensor-derived data have successfully been used in regression models for CO_2 fluxes in forests. There is a need for exploring similar relationships for other ecosystem types, such as peatlands, in order to carry out large-scale monitoring of CO_2 exchange. Failure to account for ecosystem differences is likely to result in either an over- or underestimation of CO_2 exchange at the regional or global level. The aim of this study is to assess the possibility of using satellite sensor-derived data and modeled photosynthetic photon flux density (PPFD) in regression models for CO_2 fluxes in peatlands. To achieve this, eddy covariance NEE from two Swedish peatlands were used as ground truth data. First, different environmental controls on GPP were related to modeled PPFD and MODIS LST, and then, GPP, ER, and NEE were related to various combinations of modeled PPFD, MODIS EVI, and MODIS LST.

2. Material and methods

2.1. Study sites

Two sites were used: Fäjemyr and Degerö Stormyr. Fäjemyr is a raised temperate ombrotrophic bog, surrounded by forest (see Appendix for peatland-related concepts). It is located 50 km east of the coast of Kattegat Bay in southern Sweden (56°15′N, 13°33′E) and covers about 2.9 km^2. The temperate climate has a mean (1961–1990) annual AT and precipitation of 6.2 °C (January: −2.4 °C, July: 15.1 °C) and 700 mm, respectively (Lund et al., 2007). The average (2005–2007) vegetation period is 199 days (AT > 5 °C), and the snow period is intermittent. The average (2005–2007) water table depth (WTD) is 16 cm below the surface. Peat has accumulated to the depth of about 5 m. Scattered dwarf pines (*Pinus sylvestris* L.) grow on the drier patches. Dominant vascular plant species on the hummocks are dwarf shrubs (*Calluna vulgaris* L. Hull and *Erica tetralix* L.). Sedges (mainly *Eriophorum vaginatum* L.) are common in the lawns and carpets. *Sphagnum* mosses (mainly *S. magellanicum* Brid. and *S. rubellum* Wils.) constitute the bottom layer of the lawns and carpets. Lund et al. (2009b) estimated the proportions of the hummocks, lawns/carpets, and hollows to 13%, 83%, and 4%, respectively. The moss cover was estimated to 60%. Lindroth et al. (2007) estimated the leaf area index (LAI) to about 1. The eddy covariance tower is located about 250 m from the bog edge, and the eddy covariance system, consisting of a closed-path infrared gas analyzer (IRGA, Li-Cor 6262, Li-Cor Inc, USA) and a three-dimensional sonic anemometer (Gill R3, Gill Instruments, UK), is mounted 3.4 m above the ground. Further information on site and instrumentation details can be found in Lund et al. (2007).

Degerö Stormyr (only "Degerö" in this text) is a boreal oligotrophic minerotrophic fen, surrounded by forest. It is located 70 km west of

Bothnian Bay in northern Sweden (64°11′N, 19°33′E) and covers about 6.5 km^2. The climate is cold temperate humid with a mean (1961–1990) annual AT and precipitation of 1.2 °C (January: −12.4 °C, July: 14.7 °C) and 523 mm, respectively (Nilsson et al., 2008; Sagerfors et al., 2008). The average (2001–2002 and 2005) vegetation period is 155 days (AT > 5 °C), and the snow period is 6 months long. The average (2001–2002 and 2005) WTD is 8 cm below the surface. The peatland consists of a rather complex system of interconnected smaller mires divided by islets and ridges (Nilsson et al., 2008; Sagerfors et al., 2008). Peat has accumulated to the depth of 3–4 m. The vascular plant community is dominated by sedges and dwarf shrubs (*Eriophorum vaginatum* L., *Trichophorum cespitosum* L. Hartm., *Vaccinium oxycoccos* L., *Andromeda polifolia* L., and *Rubus chamaemorus* L.). *Sphagnum* mosses dominate the hummocks, lawns, and carpets (hummocks: *S. fuscum* Schimp. Klinggr. and *S. rubellum* Wils., lawns: *S. balticum* Russ. C. Jens. and *S. lindbergii* Schimp., carpets: *S. majus* Russ. C. Jens.). Hummocks and hollows are uncommon, while lawns and carpets dominate. Lindroth et al. (2007) estimated LAI to about 1. The eddy covariance tower is located about 250 m from the fen edge, and the eddy covariance system, consisting of a closed-path infrared gas analyzer (IRGA, Li-Cor 6262, Li-Cor Inc, USA) and a three-dimensional sonic anemometer (Gill R2, Gill Instruments, UK), is mounted 1.8 m above the ground. Further information on site and instrumentation details can be found in Nilsson et al. (2008) and Sagerfors et al. (2008).

2.2. NEE, GPP, ER, and other environmental variables

The eddy covariance data covers two-and-a-half years at Fäjemyr (August 2005 to December 2007) and three years at Degerö (January 2001 to December 2002 and January to December 2005). For both sites, the measurements provided half-hourly values of NEE, incoming PPFD, AT, WTD, and vapour pressure deficit (VPD), where VPD was calculated from AT and relative humidity. Only daytime values were used for PPFD, AT, WTD, and VPD, since they were treated as GPP controls and photosynthesis is inactive during nighttime. Daytime values were selected as values when PPFD was above 10 μmol m^{-2} s^{-1}. The partitioning of NEE into GPP and ER was done using publicly available algorithms (http://www.bgc-jena.mpg.de/bgc-mdi/html/eddyproc/EddyInputForm.html). This partitioning method is based on the exponential dependency of nighttime ER on nighttime AT (Lloyd & Taylor, 1994) and is described in detail by Reichstein et al. (2005). Daytime ER is then derived by driving the exponential relationship with daytime AT, and GPP is calculated from NEE and ER. All variables were averaged for 16-day periods to match the corresponding MODIS composite periods. However, there is an apparent circularity in relating GPP estimated from AT to AT itself, and therefore, another already available data set of GPP (Lindroth et al., 2007) was employed for Fäjemyr from early April to late October 2007. The partitioning method used for this data set is based on the parameterization of an exponential regression function for two-week periods with NEE as the dependent and PPFD as the independent variable (Falge et al., 2001; Lindroth et al., 2007). Then, GPP is estimated by driving the fitted function for NEE with PPFD and subtracting the corresponding ER. The interchangeability of the 16-day averages of these two time series of GPP was checked by a linear regression with GPP estimated from AT as independent variable. Since the coefficient of determination (R^2) was as high as 0.99, the root mean square error (RMSE) as low as 0.11 g C m^{-2} day^{-1}, and the slope coefficient as close to one as 0.95 (the intercept was −0.0084 g C m^{-2} day^{-1}), GPP and ER from nighttime AT were used in the further analyses.

It should be noted that the two versions of GPP were autocorrelated seasonal variables and that the underlying assumptions of linear regression analysis were not completely fulfilled. This was true for all linear regressions in this study. In all cases, residual plots clearly showed that the errors were interdependent and that the error variances were not constant across observations (heteroscedasticity). Therefore, only R^2 and RMSE values, without any significance levels, are presented in the results.

2.3. Modeled incoming PPFD

The Swedish Meteorological and Hydrological Institute (SMHI) runs an operational mesoscale radiation model system named STRÅNG (Landelius et al., 2003). This model system produces radiation data covering Scandinavia and the Baltic Sea region with a resolution of about 11 km. Data is available on Internet (http://www.smhi.se/strang) where radiation quantities are interpolated to the position specified by lat-long coordinates using a bilinear method. STRÅNG-modeled PPFD ($PPFD_m$) was obtained for Fäjemyr and Degerö by downloading daily data and averaging it for the 16-day composite periods.

2.4. MODIS data products and field-measured NDVI

Single grid cell subsets from the Terra/MODIS 16-day 250 m collection 5 vegetation index (VI) product (MOD13Q1) were downloaded from FLUXNET (http://www.fluxnet.ornl.gov/fluxnet/index.cfm). The same time periods as for eddy covariance data were covered. The spatial extents of the cells at Fäjemyr and Degerö were compared with aerial photographs acquired from the National Land Survey of Sweden (https://butiken.metria.se/digibib/index.php). This confirmed that the chosen cells not only reference the eddy covariance towers but also cover only peatland areas and not the surrounding forest. Based on the information in Lund et al. (2007) and Sagerfors et al. (2008), also the footprints cover only peatland areas at both sites. The prevailing wind direction at Fäjemyr is from the southwest with about 90% of the flux emanating from within 200 m (Lund et al., 2007). Therefore, the cell where the eddy covariance tower is situated in the northeast corner largely overlaps the footprint. Also, the cell at Degerö largely overlaps the modeled footprint in Sagerfors et al. (2008). To extract the seasonality and reduce random noise, the time series of original MODIS NDVI ($NDVI_M$) and EVI (EVI_M) were smoothed using local double logistic curve fits in the TIMESAT software (Jönsson & Eklundh, 2002; Jönsson & Eklundh, 2004). In the evaluation study by Hird & McDermid (2009), it was concluded that the highly competitive methods in TIMESAT preserve the signal integrity to a great extent. Based on the usefulness information of the MOD13Q1 quality data, higher weights were assigned to data points with higher quality and lower weights to those with lower quality. For each site, TIMESAT-smoothed NDVI ($NDVI_{ts}$) was plotted against smoothed EVI (EVI_{ts}) to find out if there was a saturation effect in $NDVI_{ts}$ (Huete et al., 2002).

Single grid cell subsets from both the Terra/MODIS and Aqua/MODIS 8-day 1 km collection 5 LST products (MOD11A2 and MYD11A2) were also downloaded from FLUXNET. Since these two products contain data only for the 8-day composite periods, daytime and diurnal LST were derived for the 16-day composite periods. First, MOD11A2 and MYD11A2 daytime LST were averaged within the same 8-day composite periods. Second, two consecutive periods were averaged to derive daytime LST (LST_d) for the 16-day composite period. The same procedure was employed for nighttime LST, and by the subsequent averaging of 16-day day- and nighttime LST, diurnal LST (LST_{di}) was derived. However, only MOD11A2 was used for Degerö, since MYD11A2 is not produced for the whole time period needed. For both sites, single cells not referencing the eddy covariance tower positions were chosen. At Fäjemyr, the cell borders the north edge of the eddy covariance tower cell, and at Degerö it borders the northwest corner. These offsets were chosen to maximize the area of peatland covered by the 1 km cells, which resulted in more than 50% peatland area, the rest being forest.

Although the entire 250 m MODIS VI grid cells cover only peatland, one could question if the data have the same seasonality and amplitude as field-measurements. Possible adjacency effects in the MODIS

data and scale differences between the grid cells and field-measurements motivate this question. Therefore, time series of $NDVI_M$ and $NDVI_{ts}$ were plotted together with field-measured NDVI ($NDVI_{fm}$). The time series of $NDVI_{fm}$ were obtained at Fäjemyr from hemispherical-directional reflectance measurements in the wavelength interval from blue to NIR with an Analytical Spectral Devices HandHeld spectrometer (ASD HH, ASD Inc., USA) These measurements were made around noon during clear and stable weather conditions, once every three weeks from early April to late October 2007. The ASD HH has a bare fibre field of view (FOV) of 25° and a sampling interval of 1.6 nm in the spectral range of 325–1075 nm. By mounting the instrument downwards on a tripod, the measurements were made at four sampling plots, which were chosen to collectively represent the peatland vegetation composition (except for dwarf pines). The bare fibre of the ASD HH was placed 0.75 m above the surface, and by pointing it at the same spots at each measurement date, the composition of the measured vegetation was held constant. One inventory was made within the plots and resulted in 11% sedges, 32% shrubs, and 57% *Sphagnum* mosses. For each measurement, both white reference (Spectralon, Labsphere, USA) and dark scans were taken and ten spectral scans were averaged. Each plot was measured five times, and the five spectral signatures were averaged in the post-processing of data. These four sampling plot averages were averaged once again to obtain spectral signatures representative of the vegetation composition. Averaging scans and spectral signatures also served the purpose of reducing random noise in the measurements (ASD Inc., 2000). To find out how the spectral signatures developed over time and where the NIR and red spectral bands are located within the signature shapes, four of them were plotted in the same graph. Finally, weighted averages were calculated from the reflectance values spanning the MODIS red (620–670 nm) and NIR (841–876 nm) bands, and from these averages, $NDVI_{fm}$ was calculated. The weights were inferred from the spectral response functions of the MODIS red and NIR bands. To rule out the possibility that the assembly of the instrument was causing large errors on its own, the whole sequence of mounting and dismounting the instrument was repeated for twenty-eight measurements of NDVI at one of the sampling plots and resulted in a standard deviation as low as 0.0064 (mean value of 0.77).

2.5. Regression models for GPP, ER, and NEE

The sign convention adopted in this study follows Baldocchi et al. (2001), meaning that negative fluxes are transfers to the biosphere (e.g. GPP), while positive fluxes are transfers to the atmosphere (e.g. ER). In their study of CO_2 exchange in peatlands, including Fäjemyr and Degerö, Lindroth et al. (2007) used linear regression to investigate the dependency of GPP on the same environmental variables as studied here (PPFD, AT, WTD, and VPD). Careful attention was given to the correlation between the environmental variables themselves. Sims et al. (2008) used this correlation between the environmental variables (PPFD, AT, VPD, and EVI) to find a proxy variable that was related to all other variables. Also, if a certain variable turned out to be largely independent, it was assumed to contain additional information. This concept was applied here, and it was found that both $PPFD_m$ and LST_d were related to the GPP controls: PPFD, AT, WTD, and VPD, but less in EVI_{ts}. Based on scatter plots, linear regression was used for PPFD, AT, and EVI_{ts}, while exponential regression was used for WTD and VPD. Since photosynthesis is inactive when the air temperature is below the freezing point, only data when both LST_d and AT were above the approximate freezing point of 0 °C were used in these relationships. Because of these findings, GPP was related to each of $PPFD_m$ and LST_d multiplied with EVI_{ts}:

$$GPP = aEVI_{ts}PPFD_m + b \tag{2}$$

$$GPP = aEVI_{ts}LST_d + b \tag{3}$$

It could be argued that it would have been more correct to force the regression line through the origin. However, this requires scaling EVI_{ts} so that GPP is 0 when scaled EVI_{ts} is 0, and the aim of this study can be fulfilled without this procedure.

Not only GPP but also ER has to be modeled to obtain NEE from MODIS data. The Lloyd & Taylor (1994) equation was developed to describe soil respiration in a number of different ecosystems, including forests and peatlands. Lindroth et al. (2008) used it for ER in forest ecosystems and Lindroth et al. (2007) used it for peatlands, including Fäjemyr and Degerö. In this study, the equation was used to model ER by LST_{di}:

$$ER = R_{10}e^{308.56\left(\frac{1}{56.02} - \frac{1}{LST_{di} + 273.15 - 227.13}\right)}, \tag{4}$$

where R_{10} is the respiration rate at 10 °C and LST_{di} is in Celsius degrees. Diurnal LST is chosen as the independent variable, since respiration processes are active both during day- and nighttime.

Once ER is derived, NEE can be estimated by addition of its components (GPP is negative and ER is positive). Although this is one way to proceed, a multiple exponential regression model was employed in order to find out how strongly NEE can be directly related to the variables used in the relationships of GPP and ER:

$$NEE = ae^{308.56\left(\frac{1}{56.02} - \frac{1}{LST_{di} + 273.15 - 227.13}\right)} + bEVI_{ts}PPFD_m + c, \tag{5}$$

where NEE is expressed as the combination of Eq. (2) and Eq. (4). Similar to when GPP was calculated, only data when LST_d and AT were above 0 °C were used. Only the combination of $PPFD_m$ and EVI_{ts} was chosen in this direct approach.

To find out how well the seasonality of the modeled GPP, ER, and NEE (Eqs. (2)–(5)) correspond to the measured CO_2 fluxes at Fäjemyr and Degerö, modeled and measured time series were plotted in the same graphs. Also, to find out how different the results would be, if the CO_2 fluxes at Fäjemyr were modeled with the regression coefficients for Degerö and vice versa, both Fäjemyr and Degerö were modeled with the regression coefficients for each site. Averages and standard deviations of measured and modeled values were then calculated for the time periods covered for each site (Fäjemyr: 2005–2007, Degerö: 2001–2002 and 2005).

3. Results

3.1. Seasonality in NDVI and EVI

The seasonality of MODIS VI was extracted and random noise reduced by the local double logistic curve fits in TIMESAT (Fig. 1). The large scatter in $NDVI_M$ during the second winter 2006/2007 at Fäjemyr consists of data points with low MODIS usefulness quality. Since these data points have been assigned lower weights in the smoothing procedure, they only have a minor influence on the curve fit. The small ridge-like curves in $NDVI_{ts}$ and EVI_{ts} between 2002 and 2005 for Degerö are artifacts of the two separate smoothing procedures employed for the two time periods of 2001–2002 and 2005. Important is the summertime leveling of $NDVI_{ts}$ at both sites, which indicates a saturation effect in NDVI, compared to EVI. This is confirmed by Fig. 2 where the saturation effect is quite clear in the scatter plot of $NDVI_{ts}$ and EVI_{ts}. Smoothed instead of original data were plotted, because smoothed data were used in the further analyses. The saturation effect and the slightly stronger relationships found between GPP and EVI_{ts} for Fäjemyr and Degerö (EVI_{ts}: $R^2 = 0.37$ and 0.45, $NDVI_{ts}$: $R^2 = 0.26$ and 0.36) were the reasons for choosing EVI_{ts} in the analyses. For Fäjemyr, it was confirmed that there is a close resemblance between MODIS and field-measured NDVI (Fig. 3), supporting that MODIS VI represents the peatland vegetation. In spite of the pronounced outlier in $NDVI_M$, there is a close resemblance in seasonality and amplitude with

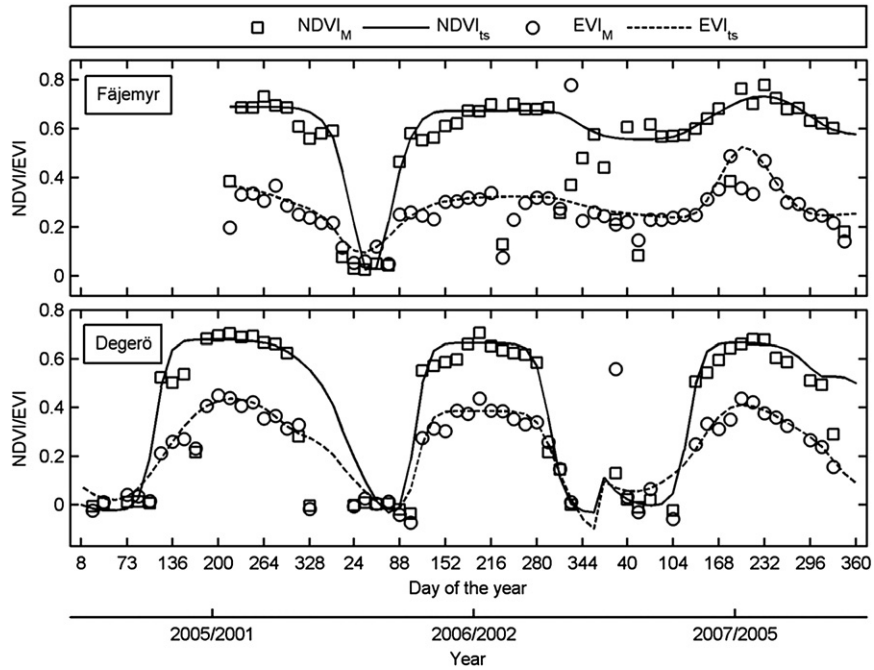

Fig. 1. Time series of $NDVI_M$, EVI_M, $NDVI_{ts}$, and EVI_{ts} for Fäjemyr (2005–2007) and Degerö (2001–2002 and 2005). Off note are the small ridge-like curves in $NDVI_{ts}$ and EVI_{ts} between 2002 and 2005 for Degerö. These are artifacts of the two separate smoothing procedures for the time periods of 2001–2002 and 2005. Abbreviations: EVI_M, MODIS enhanced vegetation index; EVI_{ts}, TIMESAT-smoothed enhanced vegetation index; $NDVI_M$, MODIS normalized difference vegetation index; $NDVI_{ts}$, TIMESAT-smoothed normalized difference vegetation index.

$NDVI_{fm}$. By reducing noise, the TIMESAT processing improved the similarity between $NDVI_{ts}$ and $NDVI_{fm}$. The seasonal increase in NDVI is a result of the increase in the difference between the NIR and red reflectance values (Fig. 4). Since NDVI was calculated from the MODIS bands, the red band (620–670 nm) is located just before the wavelength of maximum absorption, while the NIR band (841–876 nm) is located on the upward slope of maximum reflectance.

3.2. $PPFD_m$ and LST_d as proxy variables

The R^2 values in Table 1 show that both $PPFD_m$ and LST_d can serve as proxy variables for the major controls on GPP (PPFD, AT, WTD, and VPD). For Fäjemyr, the controls on GPP, except for EVI_{ts}, were related to both $PPFD_m$ and LST_d. This also suggests that EVI_{ts} may contribute with additional information about the temporal vegetation development to $PPFD_m$ and LST_d. However, the results are not equally consistent for Degerö where there were weak relationships between GPP and $PPFD_m$ and between AT and $PPFD_m$, and almost no relationship between WTD and $PPFD_m$. In addition, PPFD and WTD were only weakly related to LST_d. On the other hand, the time series of GPP, AT, and PPFD were slightly truncated during the growing seasons in 2001 and 2005, because of a few missing summertime data points, and this probably weakened the relationships. This assumption was confirmed by the stronger relationship found between GPP and $PPFD_m$ when only non-truncated data from 2002 were used ($R^2 = 0.54$). Also, the weak relationships between WTD and the proxy variables could be a less important argument against using $PPFD_m$ and LST_d as proxy variables, since GPP was found to be weakly related to

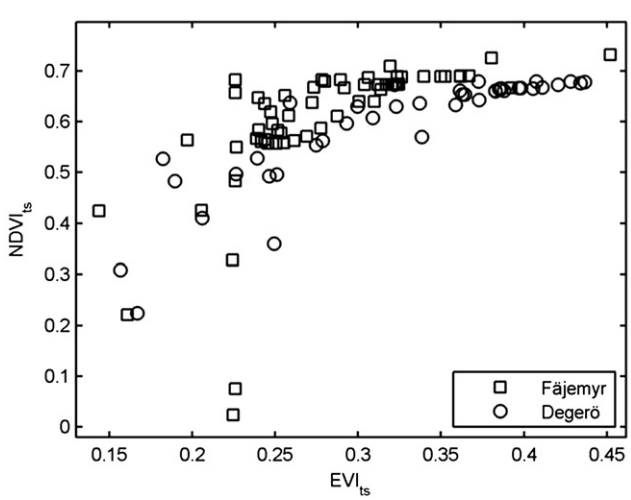

Fig. 2. Scatter plot of $NDVI_{ts}$ and EVI_{ts} for Fäjemyr and Degerö. Abbreviations: EVI_{ts}, TIMESAT-smoothed enhanced vegetation index; $NDVI_{ts}$, TIMESAT-smoothed normalized difference vegetation index.

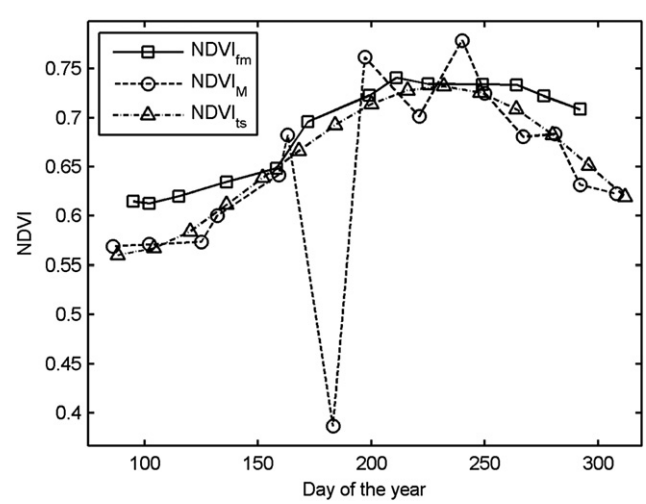

Fig. 3. Time series of $NDVI_{fm}$, $NDVI_M$, and $NDVI_{ts}$ for Fäjemyr. For $NDVI_M$, the MODIS composite day of the year is used, and for $NDVI_{ts}$, the day of the year at the center of the composite period is used. Abbreviations: $NDVI_{fm}$, field-measured normalized difference vegetation index; $NDVI_M$, MODIS normalized difference vegetation index; $NDVI_{ts}$, TIMESAT-smoothed normalized difference vegetation index.

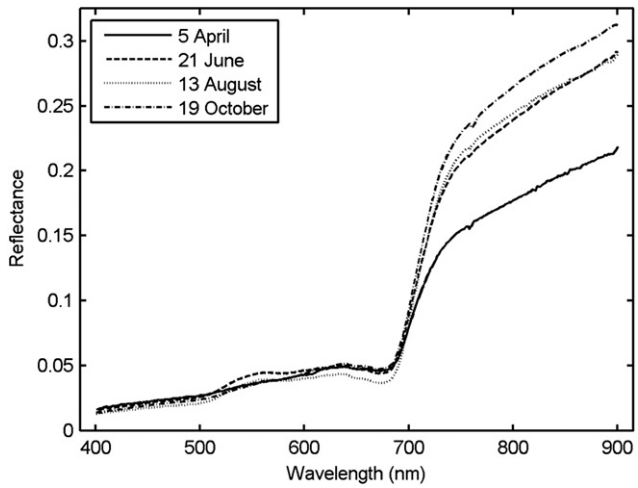

Fig. 4. Spectral signatures measured at Fäjemyr with an Analytical Spectral Devices HandHeld spectrometer (ASD HH, ASD Inc., USA). The wavelength range is limited to 400–900 nm, because of noise in lower and higher wavelengths.

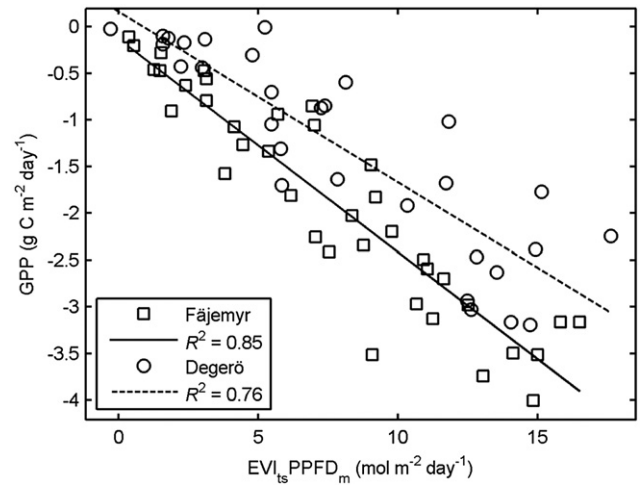

Fig. 5. Linear regressions for GPP at Fäjemyr and Degerö against $EVI_{ts}PPFD_m$ (Eq. (2)). Abbreviations: EVI_{ts}, TIMESAT-smoothed enhanced vegetation index; GPP, gross primary productivity; $PPFD_m$, modeled photosynthetic photon flux density.

WTD ($R^2 = 0.19$). Similar to Fäjemyr, the relationships between EVI_{ts} and the proxy variables were fairly weak, indicating that EVI_{ts} may contribute with additional information about the temporal vegetation development.

3.3. Regression results for GPP, ER, and NEE

Strong relationships were found between GPP and the products of each of the proxy variables and EVI_{ts} (Figs. 5–6 and Table 2). It is interesting that the product of EVI_{ts} and $PPFD_m$ had the slightly higher R^2 values of 0.85 for Fäjemyr and 0.76 for Degerö, compared to EVI_{ts} and LST_d. These values were higher even though GPP was strongly related to LST_d itself (Table 1). It seems that EVI_{ts} contributes with more complementary information to $PPFD_m$ than to LST_d. This is reasonable, because the linear dependency of FAPAR on VI makes the relationship between GPP and the product of VI and PPFD an approximation of the LUE model. The weaker relationships for Degerö were probably caused by the absence of a few summertime data points for the related variables. This explanation also applies to ER. The fitting of the Lloyd & Taylor (1994) equation to ER and LST_{di} resulted in the high R^2 value of 0.89 for Fäjemyr and the slightly lower 0.83 for Degerö (Fig. 7 and Table 3). Even though NEE is the sum of GPP and ER, the direct model with NEE in the multiple exponential relationship to LST_{di} and the product of EVI_{ts} and $PPFD_m$ was applied.

Table 1
Coefficient of determination values (R^2) for environmental variables at Fäjemyr and Degerö against $PPFD_m$ and LST_d. The relationships are linear except those with WTD and VPD, which are exponential. A minus sign within parentheses means that the relationship has a descending slope.

	GPP	PPFD	AT	WTD	VPD	EVI_{ts}
Fäjemyr						
$PPFD_m$	(−) 0.69	0.98	0.64	(−) 0.79[b]	0.81[a]	0.058
LST_d	(−) 0.81	0.79	0.86	(−) 0.85[b]	0.87[a]	0.18
Degerö						
$PPFD_m$	(−) 0.40	0.98	0.37	(−) 0.14[b]	0.71[a]	0.017
LST_d	(−) 0.64	0.36	0.79	(−) 0.33[b]	0.76[a]	0.44

Abbreviations: AT, air temperature; EVI_{ts}, TIMESAT-smoothed enhanced vegetation index; GPP, gross primary productivity; LST_d, daytime MODIS land surface temperature; $PPFD_m$, modeled photosynthetic photon flux density; PPFD, photosynthetic photon flux density; VPD, vapour pressure deficit; WTD, water table deficit.
[a] Equation: $y = ae^{bx}$.
[b] Equation: $y = ae^{bx} + c$.

This resulted in the higher R^2 value of 0.81 for Fäjemyr and 0.73 for Degerö (Table 4). In spite of the exponential component in Eq. (5), the fitted sloping surfaces were rather planar (not shown in any figures). However, only data from when both AT and LST_d were above 0 °C were used in these relationships, and in Fig. 7, it can be seen that the upper parts of the graphs have weaker curvatures than if the entire temperature range would have been used. Of note are the RMSE values of 0.18 g C m^{-2} day^{-1} for Fäjemyr and 0.28 g C m^{-2} day^{-1} for Degerö (Fig. 8 and Table 4). For comparison, the averages of absolute NEE are 0.35 g C m^{-2} day^{-1} for Fäjemyr and 0.55 g C m^{-2} day^{-1} for Degerö. If NEE would have been calculated from GPP and ER, then the RMSE values would have been much higher, because of error propagation. One objection to the regression results for GPP and NEE could be that the chosen air temperature limit of 0 °C is too low, since the peatlands may still be covered by snow. While Fäjemyr has an intermittent snow period, Degerö has a snow period that is 6 months long. However, the higher air temperature limit of 5 °C was tested for Degerö, and it did not change the results enough to alter any conclusions (GPP against $EVI_{ts}PPFD_m$: $R^2 = 0.64$, NEE against LST_{di} and $EVI_{ts}PPFD_m$: $R^2 = 0.70$).

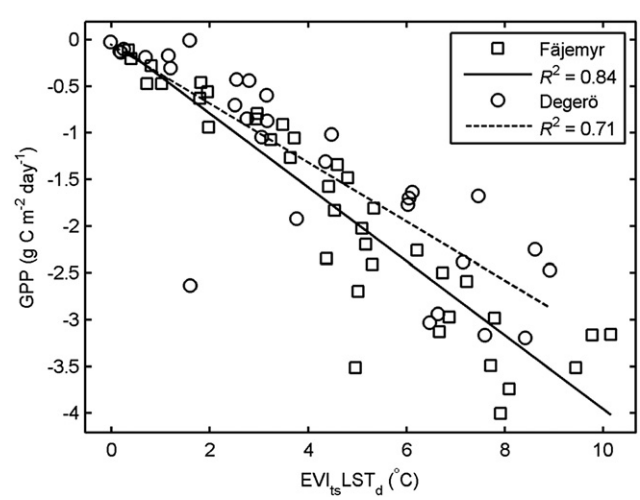

Fig. 6. Linear regressions for GPP at Fäjemyr and Degerö against $EVI_{ts}LST_d$ (Eq. (3)). Abbreviations: EVI_{ts}, TIMESAT-smoothed enhanced vegetation index; GPP, gross primary productivity; LST_d, daytime MODIS land surface temperature.

Table 2
Linear regressions for GPP (g C m^{-2} day^{-1}) at Fäjemyr and Degerö against $EVI_{ts}PPFD_m$ (mol m^{-2} day^{-1}) (Eq. (2)) and $EVI_{ts}LST_d$ (°C) (Eq. (3)).

Explained	Explanatory	Points	R^2	RMSE	Slope	Intercept
Fäjemyr						
GPP	$EVI_{ts}PPFD_m$	38	0.85	0.44	−0.23	−0.13
GPP	$EVI_{ts}LST_d$	38	0.84	0.45	−0.40	−0.0024
Degerö						
GPP	$EVI_{ts}PPFD_m$	30	0.76	0.51	−0.18	0.16
GPP	$EVI_{ts}LST_d$	30	0.71	0.56	−0.32	−0.051

Abbreviations: EVI_{ts}, TIMESAT-smoothed enhanced vegetation index; GPP, gross primary productivity; LST_d, daytime MODIS land surface temperature; $PPFD_m$, modeled photosynthetic photon flux density.

For both Fäjemyr and Degerö, there is a strong correspondence between the modeled (Eqs. (2)–(3)) and measured time series of GPP (Fig. 9). Possibly, the time series of $PPFD_m$-modeled GPP is slightly displaced in time so that it precedes measured GPP, while LST_d-modeled GPP is delayed. Also, the modeled time series of ER and NEE corresponds well to the measured CO_2 fluxes (Fig. 10). The largest under- and overestimations of GPP, ER, and NEE are found during the peak seasons. However, the displacements and under- and overestimations should be less important, if modeled CO_2 fluxes are averaged for whole years. Averages and standard deviations of measured and modeled CO_2 fluxes covering the time periods for Fäjemyr and Degerö are found in Table 5. If the regression coefficients for Fäjemyr are used for Fäjemyr and those for Degerö are used for Degerö, then there are strong similarities between measured and modeled averages. However, there are large differences if the CO_2 fluxes at Fäjemyr are modeled with the regression coefficients for Degerö, and vice versa.

4. Discussion

The results of this study show that satellite sensor-derived data and modeled PPFD can be used in regression models for estimations of CO_2 fluxes in peatlands. Both the product of EVI_{ts} and $PPFD_m$ and the product of EVI_{ts} and LST_d strongly explained GPP at Fäjemyr and Degerö. One reason for these results probably is that other controls on GPP were related to both $PPFD_m$ and LST_d. Also, ER was strongly related to LST_{di}, and based on these findings, NEE was successfully related to LST_{di} in combination with the product of EVI_{ts} and $PPFD_m$. Still, the biophysically correct way of modeling GPP would be to use

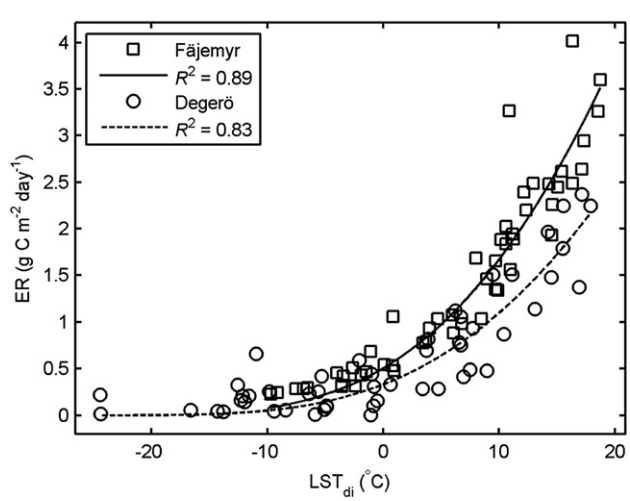

Fig. 7. Exponential regressions for ER at Fäjemyr and Degerö against LST_{di} (Eq. (4)). Abbreviations: ER, ecosystem respiration; LST_{di}, diurnal MODIS land surface temperature.

Table 3
Exponential regressions for ER (g C m^{-2} day^{-1}) at Fäjemyr and Degerö against LST_{di} (°C) (Eq. (4)).

Explained	Explanatory	Points	R^2	RMSE	R_{10}
Fäjemyr					
ER	LST_{di}	52	0.89	0.33	1.67
Degerö					
ER	LST_{di}	51	0.83	0.26	1.10

Abbreviations: ER, ecosystem respiration; LST_{di}, diurnal MODIS land surface temperature.

the LUE model together with separate estimations of ε, which is the concept implemented in the MODIS GPP product (Running et al., 2004). On the other hand, one problem with this approach in peatlands is to obtain FAPAR, since it is difficult to measure transmitted light below the water-saturated vegetation. Early in this study, incoming and reflected PPFD, measured at Fäjemyr, were used to calculate the fraction of intercepted photosynthetically active radiation (FIPAR). However, the absorption by the considerable amount of water and dead plant material made FIPAR inappropriate as an approximation of FAPAR. In a future study, another alternative may be to model FAPAR with leaf area index (LAI) as input to Beer's Law (Ahl et al., 2004; Turner et al., 2005; Conolly et al., 2009).

Despite the above-discussed limitation, the results open up the use of satellite data in regression models for GPP, of the kind already studied in forest areas (Olofsson et al., 2008; Rahman et al., 2005; Sims et al., 2006; Sims et al., 2008). In addition, the models employed here are to some extent similar to the LUE model, since the strong dependency of FAPAR on VI makes the relationship between GPP and the product of EVI_{ts} and $PPFD_m$ an approximation of the LUE model. Similarly, the relationship to the product of EVI_{ts} and LST_d is such an approximation, to the extent that temperature is related to PPFD. Also, the strong relationships between AT and LST_d at both sites indicates that LST_d can be used as a substitute for air temperature, despite the coarse resolution of 1 km and the forest coverage of nearly 50%. Even though these relationships may be restrained by air temperature differences between the peatland and the surrounding forest, it seems reasonable to assume a strong correlation between the peatland and forest air temperature. The findings by Lindroth et al. (2007), which show that GPP is related to AT at both Fäjemyr and Degerö, and the findings by Conolly et al. (2009), which show that ε is related to AT in two peatlands in Canada, support temperature as a good alternative in a GPP model. However, the product of EVI_{ts} and $PPFD_m$ was used for the GPP component in the direct approach of modeling NEE. Apart from its close similarity to the LUE model, $PPFD_m$ was a better choice, because it was interpolated to the specific positions of the eddy covariance towers. The direct NEE model also avoided the logical circularity in relating GPP partitioned by air temperature to temperature itself, since NEE is not partitioned from other variables. Another advantage was that the model resulted in much smaller errors than if NEE would have been calculated as the sum of estimated GPP and ER, because of the propagation of errors. Therefore, it may be

Table 4
Multiple exponential regressions for NEE (g C m^{-2} day^{-1}) at Fäjemyr and Degerö against LST_{di} (°C) and $EVI_{ts}PPFD_m$ (mol m^{-2} day^{-1}) (Eq. (5)).

Explained	Explanatory	Points	R^2	RMSE	a	b	c
Fäjemyr							
NEE	LST_{di} and $EVI_{ts}PPFD_m$	38	0.81	0.18	0.19	−0.097	0.42
Degerö							
NEE	LST_{di} and $EVI_{ts}PPFD_m$	37	0.73	0.28	−0.035	−0.090	0.38

Abbreviations: EVI_{ts}, TIMESAT-smoothed enhanced vegetation index; LST_{di}, diurnal MODIS land surface temperature; NEE, net ecosystem exchange; $PPFD_m$, modeled photosynthetic photon flux density.

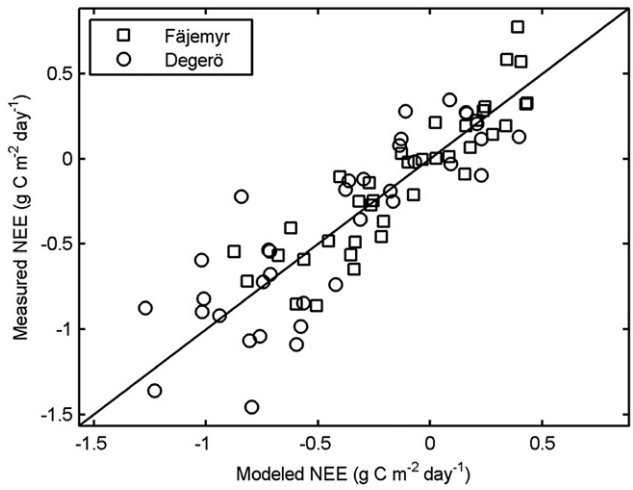

Fig. 8. Measured NEE at Fäjemyr and Degerö against modeled NEE. The coefficients for the multiple regression for NEE against LST_{di} and $EVI_{ts}PPFD_m$ were used to model NEE (Eq. (5)). Abbreviations: EVI_{ts}, TIMESAT-smoothed enhanced vegetation index; LST_{di}, diurnal MODIS land surface temperature; NEE, net ecosystem exchange; $PPFD_m$, modeled photosynthetic photon flux density.

preferred to employ a direct approach, given that NEE is the final goal of the modeling procedure.

Not only the LUE models but also the regression models for CO_2 fluxes are most likely constrained by temporal and spatial changes in ε and the regression coefficients (e.g. slope). Several studies have shown that ε not only varies temporally throughout the season but also spatially between the ecosystems and plant functional types (Ruimy et al., 1994; Turner et al., 2002; Brogaard et al., 2005; Conolly et al., 2009). Although the regression coefficients are inferred from relating CO_2 fluxes to environmental variables, it does not follow that they are constant across time and space. It is known that CO_2 fluxes vary between various peatlands (Bubier et al., 1998; Lindroth et al., 2007; Lund et al., 2009a; Aurela et al., 2009) and also between years within the sites (Aurela et al., 2004; Roulet et al., 2007; Sagerfors et al., 2008; Aurela et al., 2009). This may be explained by differences in vegetation composition (Bubier et al., 2003; Riutta et al., 2007) and changing environmental conditions, such as weather (Aurela et al., 2004; Aurela et al., 2009). Not only the environmental variables included in this study, e.g. AT and WTD, can affect the CO_2 fluxes (Lafleur et al., 2003; Lindroth et al., 2007), but also the nutrient availability is important. Bubier et al. (1998) found that NEE and ER followed the trophic sequence from oligotrophic bog to eutrophic fen of a peatland complex in Canada, indicating the importance of nutrient conditions. On the other hand, Humphreys et al. (2006) found that summertime NEE was similar for seven Canadian peatlands, despite differences in vegetation composition, nutrient availability, and WTD. In addition, GPP and ER were found to depend on VI and aboveground biomass. Even though changes in CO_2 fluxes may be captured by the environmental variables used in the model relationships, CO_2 fluxes should also depend on differences in ε and the regression coefficients, which in turn, should depend on different plant communities and environmental conditions. If applied without considering changes in ε and the regression coefficients, the LUE and regression models are correct only to the extent that ε or the coefficients are constant across time and space. The results of this study show that the regression coefficients are different between Fäjemyr and Degerö (Tables 2–4) and that there would be large differences between measured and modeled CO_2 fluxes, if Fäjemyr is modeled with the regression coefficients for Degerö, and vice versa (Table 5).

Because of the narrow red absorption bands and NIR peaks in *Sphagnum* mosses, Bubier et al. (1997) concluded that NDVI should be a poor estimator of biomass and greenness. Also, the seasonal range in NDVI should be lower, because of the smaller difference between the red and NIR reflectance in *Sphagnum* mosses. The presence of red *Sphagnum* mosses (e.g. *S. magellanicum*) at Fäjemyr and both red and brown (e.g. *S. rubellum* and *S. fuscum*) at Degerö make these arguments valid. This means that it probably is harder to find strong relationships between CO_2 fluxes and NDVI in peatlands. These

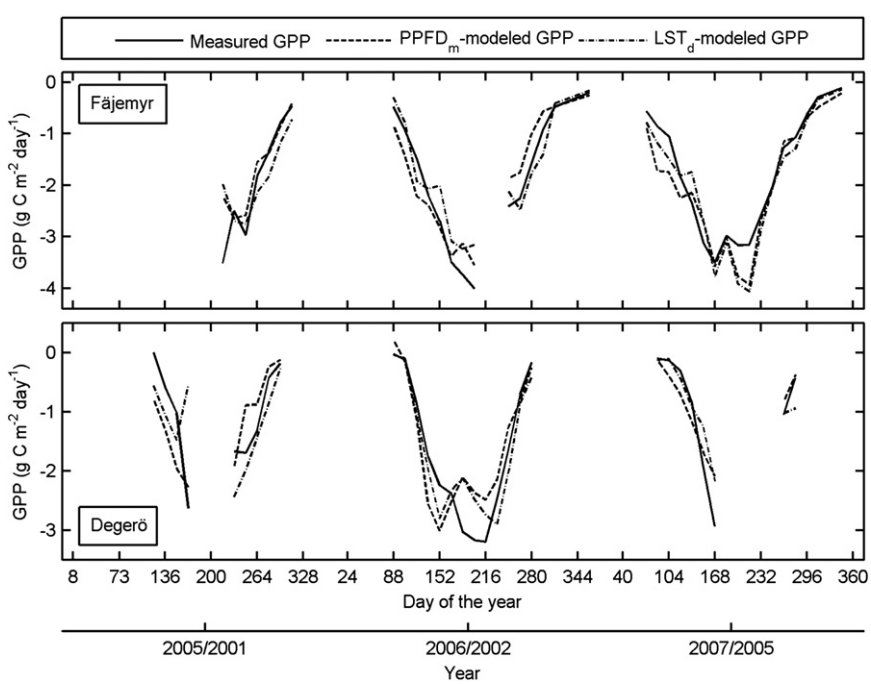

Fig. 9. Time series of measured and modeled 16-day GPP for Fäjemyr (2005–2007) and Degerö (2001–2002 and 2005). By using the regression coefficients (Table 2) derived for each site, 16-day values of GPP were modeled both from $PPFD_m$ (Eq. (2)) and LST_d (Eq. (3)). The data gaps are the result of missing data in measured or modeled GPP. Abbreviations: GPP, gross primary productivity; $PPFD_m$, modeled photosynthetic photon flux density; LST_d, daytime MODIS land surface temperature.

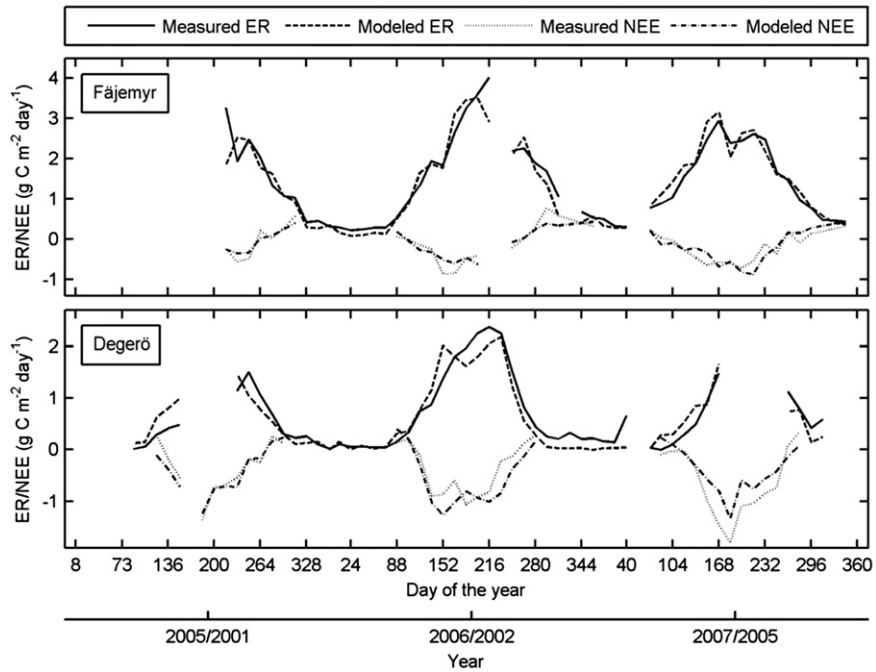

Fig. 10. Time series of measured and modeled 16-day ER and NEE for Fäjemyr (2005–2007) and Degerö (2001–2002 and 2005). By using the regression coefficients (Tables 3–4) derived for each site, 16-day values of ER (Eq. (4)) and NEE (Eq. (5)) were modeled. The data gaps are the result of missing data in measured or modeled ER and NEE. Abbreviations: ER, ecosystem respiration; NEE, net ecosystem exchange.

arguments also have implications for EVI, since it is calculated from red, NIR, and blue reflectance values. In addition, not only MODIS VI but also field-measured NDVI were calculated from the MODIS red (620–670 nm) and NIR (841–876 nm) bands, which does not seem optimal for the peatland vegetation at Fäjemyr (Fig. 4). Moving both bands to larger wavelengths would capture the maximum red absorption and maximum NIR reflectance in a better way. All measurements in this study have been made over a mixed vegetation cover of both *Sphagnum* mosses and vascular plants, and hence, it is hard to evaluate to what extent this mix of plant functional types affects the results. However, an indication of both the influence of changing regression coefficients and spectral characteristics of the vegetation on modeled CO_2 fluxes may be obtained by a comprehensive validation study against eddy covariance measurements for other years and at other sites.

From the results by Heinsch et al. (2006) and Krankina et al. (2008) it follows that the coarse resolution 1 km MOD17 product with its input of even coarser meteorological data is inappropriate for heterogeneous areas, such as peatlands. Another problem is that ε is extracted based on the 1 km MOD12Q1 land cover classification scheme without any category relevant for peatlands (Heinsch et al., 2003). This study avoided the resolution problem by using the 250 m grid cells of EVI, located within the peatlands, and modeled PPFD, interpolated to the positions of the eddy covariance towers. Also, it seems reasonable that the air temperature seasonality within peatlands resembles the surrounding forests, hence allowing 1 km LST to be used as a substitute for air temperature. However, Tan et al. (2006) shows that the MODIS gridding process in combination with the geolocation error and the point spread function (PSF) of the sensor observations results in an average overlap of only 30% between the grid cells and the true observations. It is emphasized that this has strong implications for the use of reference data in validation procedures, because of the mismatch between the observations and field measurements. The implications for this study are not only possible mismatches between the observations and the eddy covariance tower positions, but also that the observations may include the surrounding forests. It was suggested by Tan et al. (2006) that information on the observation dimensions and the offsets between the cells and observations should be included in validations to guarantee quality. One possible solution for peatlands

Table 5
Averages (Avg) and standard deviations (Std) of measured and modeled GPP (g C m^{-2} day^{-1}), ER (g C m^{-2} day^{-1}), and NEE (g C m^{-2} day^{-1}) for Fäjemyr and Degerö. Time series of 16-day values were averaged and standard deviations were calculated for the time periods covered for each site (Fäjemyr: 2005–2007, Degerö: 2001–2002 and 2005). Sixteen-day GPP, ER, and NEE were modeled with Eqs. (2)–(5). Both Fäjemyr and Degerö were modeled with the regression coefficients (Tables 2–4) for each site.

	Avg GPP Eq. (2)	Std GPP Eq. (2)	Avg GPP Eq. (3)	Std GPP Eq. (3)	Avg ER Eq. (4)	Std ER Eq. (4)	Avg NEE Eq. (5)	Std NEE Eq. (5)
Fäjemyr								
Measured	−1.86	1.16	−1.86	1.16	1.44	1.01	−0.12	0.41
Fäjemyr coeff	−1.88	1.08	−1.89	1.07	1.40	1.01	−0.12	0.37
Degerö coeff	−1.21	0.84	−1.56	0.86	0.92	0.66	−0.25	0.38
Degerö								
Measured	−1.30	1.06	−1.30	1.06	0.63	0.66	−0.45	0.55
Degerö coeff	−1.31	0.91	−1.33	0.92	0.59	0.64	−0.45	0.48
Fäjemyr coeff	−2.01	1.17	−1.60	1.15	0.90	0.97	−0.24	0.40

Abbreviations: ER, ecosystem respiration; GPP, gross primary productivity; NEE, net ecosystem exchange.

would be to use the offset information for daily reflectance values and pick out values for observations close enough to the eddy covariance tower positions. Furthermore, the Spatial and Temporal Adaptive Reflectance Fusion Model (STARFM), developed by Gao et al. (2006), has shown positive results for downscaling MODIS reflectance data to the Landsat 30 m resolution. In this way, the temporal resolution is preserved, while increasing the spatial resolution. If some appropriate downscaling procedure can be used, the resolution will be high enough to pick out grid cells that are not only located within the peatlands, but also within the eddy covariance tower footprints. In addition to the influence of changing regression coefficients and the spectral characteristics on modeled CO_2 fluxes, as discussed above, there is a need to solve spatial problems in order to improve the performance of using satellite sensor-derived data in regression modeling of CO_2 fluxes in peatlands.

5. Conclusions

(1) This study shows that regression models driven by satellite sensor-derived data and modeled PPFD can be used to estimate CO_2 fluxes in peatlands. Strong relationships were found between GPP and the product of MODIS EVI and modeled PPFD, as well as the product of MODIS EVI and MODIS LST. Also, ER was strongly related to MODIS LST, and NEE was largely explained by MODIS LST in combination with the product of MODIS EVI and modeled PPFD.

(2) Several GPP controls (PPFD, AT, WTD, and VPD) were related to modeled PPFD and also to MODIS LST. Therefore, modeled PPFD and MODIS LST can serve as proxy variables for the GPP controls. Since MODIS EVI was weakly related to the proxy variables, MODIS EVI may provide additional information in relation to the CO_2 fluxes. This serves as an explanation to the strong relationships found for GPP and NEE.

(3) The LUE and regression models are likely to be constrained by temporal and spatial changes in ε and the regression coefficients. Differences in ε and the coefficients should depend on different plant communities and environmental conditions, which means that they are not constant across time and space. At the temporal and spatial scale of this study, the regression models are correct only to the extent that ε or the coefficients are constant.

(4) Problems related to the application of coarse resolution MODIS data in smaller peatland areas need to be solved. Not only is there a need for considering the grid cell resolution, but the MODIS gridding process that results in a small average overlap between the cell and the true observation also needs to be taken into account. One possible way is to use information on the offset between the cell and the observations to pick out reflectance values for observations close enough to the eddy covariance tower positions. Also, some appropriate downscaling procedure may be used to increase the spatial resolution to match the peatland area and eddy covariance tower footprints.

Acknowledgements

This study was funded through a project grant from the Swedish National Space Board (SNSB). The globally integrating carbon flux measurement network, FLUXNET, provided subsets of MODIS data. Modeled STRÅNG data were provided by the Swedish Meteorological and Hydrological Institute (SMHI) and produced with support from the Swedish Radiation Safety Authority (SRSA) and the Swedish Environmental Protection Agency (SEPA). Special thanks are given to Professor Per Jönsson at Malmö University for answering specific questions on curve fitting, to Professor Anders Lindroth at Lund University for discussing problems related to flux partitioning, and to Lecturer Jonathan Seaquist for proofreading the manuscript.

Appendix A. Abbreviations, symbols, and peatland-related concepts

Table A. Abbreviations and symbols and their descriptions. The abbreviations and symbols in italics are only mentioned in the text and not used in the study itself.

Abbreviation or symbol	Description
APAR	Absorbed photosynthetically active radiation (W m^{-2} day^{-1})
AT	Air temperature (°C)
ER	Ecosystem respiration (g C m^{-2} day^{-1})
EVI_{ts}	TIMESAT-smoothed MODIS enhanced vegetation index
ε	Light use efficiency factor (g C W^{-1})
FAPAR	Fraction of absorbed photosynthetically active radiation
FIPAR	Fraction of intercepted photosynthetically active radiation
GPP	Gross primary productivity (g C m^{-2} day^{-1})
LAI	Leaf area index
LST_d	Daytime MODIS land surface temperature (°C)
LST_{di}	Diurnal MODIS land surface temperature (°C)
LUE	Light use efficiency
$NDVI_{fm}$	Field-measured normalized difference vegetation index
$NDVI_M$	MODIS normalized difference vegetation index
$NDVI_{ts}$	TIMESAT-smoothed MODIS normalized difference vegetation index
NEE	Net ecosystem exchange (g C m^{-2} day^{-1})
NPP	Net primary productivity (g C m^{-2} day^{-1})
PAR	Photosynthetically active radiation (W m^{-2} day^{-1})
PPFD	Photosynthetic photon flux density (mol m^{-2} day^{-1})
$PPFD_m$	Modeled photosynthetic photon flux density (mol m^{-2} day^{-1})
VI	Vegetation index
VPD	Vapour pressure deficit (kPa)
WTD	Water table depth (cm)

Table B. Peatland-related concepts and their definitions. Modified from Rydin & Jeglum (2006).

Concept	Definition
Carpet	Peatland vegetation dominated by bryophytes and with a sparse cover of cyperaceous plants. The vegetation layer is leveled at 5 cm below to 5 cm above the water table.
Hollow	Depression in a peatland that is characterized by an alternating microtopography.
Hummock	Peatland vegetation leveled at 20–50 cm above the lowest surface level. The vegetation layer consists of mosses, lichens, and dwarf shrubs.
Lawn	Peatland vegetation dominated by graminoids and with a diversified bryophyte layer. The vegetation layer is leveled at 5 to 20 cm above the water table.
Minerotrophic peatland/Fen	Peatland with an inflow of water and nutrients from mineral soils.
Oligotrophic peatland	Nutrient-poor peatland
Ombrotrophic peatland/Bog	Peatland with water and nutrients coming only from precipitation, dust, sea-spray, and airborne deposition.
Peatland	Peat-covered terrain with a minimum peat depth of 30 or 40 cm.

References

Ahl, D. E., Gower, S. T., Mackay, D. S., Burrows, S. N., Norman, J. M., & Diak, G. R. (2004). Heterogeneity of light use efficiency in a northern Wisconsin forest: Implications for modeling net primary production with remote sensing. *Remote Sensing of Environment*, *93*, 168−178.

ASD Inc. (2000). *FieldSpec® Pro User's Guide* (pp. 1−90). Boulder: Analytical Spectral Devises Inc.

Aselmann, I., & Crutzen, P. J. (1989). Global distribution of natural freshwater wetlands and rice paddies, their net primary productivity, seasonality and possible methane emissions. *Journal of Atmospheric Chemistry*, *8*, 307−358.

Asrar, G., Fuchs, M., Kanemasu, E. T., & Hatfield, J. L. (1984). Estimating absorbed photosynthetic radiation and leaf area index from spectral reflectance in wheat. *Agronomy Journal*, *76*, 300−306.

Asrar, G., Myneni, R. B., & Choudhury, B. J. (1992). Spatial heterogeneity in vegetation canopies and remote sensing of absorbed photosynthetically active radiation: A modeling study. *Remote Sensing of Environment*, *41*, 85−103.

Aubinet, M., Grelle, A., Ibrom, A., Rannik, Ü., Moncrieff, J., Foken, T., et al. (2000). Estimates of the annual net carbon and water exchange of forests: The EUROFLUX methodology. *Advances in Ecological Research*, *30*, 113−175.

Aurela, M., Laurila, T., & Tuovinen, J. -P. (2004). The timing of snow melt controls the annual CO_2 balance in a subarctic fen. *Geophysical Research Letters*, *31*, L16119. doi:10.1029/2004GL020315

Aurela, M., Riutta, T., Laurila, T., Tuovinen, J. -P., Vesala, T., Tuittila, E. -S., et al. (2007). CO_2 exchange of a sedge fen in southern Finland — The impact of a drought period. *Tellus B*, *59*, 826−837.

Aurela, M., Lohila, A., Tuovinen, J. -P., Hatakka, J., Riutta, T., & Laurila, T. (2009). Carbon dioxide exchange on a northern boreal fen. *Boreal Environment Research*, *14*, 699−710.

Baldocchi, D. D., Falge, E., Gu, L., Olson, R., Hollinger, D., Running, S., et al. (2001). FLUXNET: A new tool to study the temporal and spatial variability of ecosystem-scale carbon dioxide, water vapor, and energy flux densities. *Bulletin of the American Meteorological Society*, *82*, 2415−2434.

Baldocchi, D. D. (2003). Assessing the eddy covariance technique for evaluating carbon dioxide exchange rates of ecosystems: Past, present and future. *Global Change Biology*, *9*, 479−492.

Brogaard, S., Runnström, M., & Seaquist, J. W. (2005). Primary production of Inner Mongolia, China, between 1982 and 1999 estimated by a satellite data-driven light use efficiency model. *Global Planet Change*, *45*, 313−332.

Bryant, R. G., & Baird, A. J. (2003). The spectral behaviour of *Sphagnum* canopies under varying hydrological conditions. *Geophysical Research Letters*, *30*, 1134−1137.

Bubier, J. L., Rock, B. N., & Crill, P. M. (1997). Spectral reflectance measurements of boreal wetland and forest mosses. *Journal of Geophysical Research*, *102*, 29483−29494.

Bubier, J. L., Crill, P. M., Moore, T. R., Savage, K., & Varner, R. K. (1998). Seasonal patterns and controls on net ecosystem CO_2 exchange in a boreal peatland complex. *Global Biogeochemical Cycles*, *12*, 703−714.

Bubier, J. L., Bhatia, G., Moore, T. M., Roulet, N. T., & Lafleur, P. M. (2003). Spatial and temporal variability in growing-season net ecosystem carbon dioxide exchange at a large peatland in Ontario, Canada. *Ecosystems*, *6*, 353−367.

Chen, J. M. (1996). Canopy architecture and remote sensing of the fraction of photosynthetically active radiation absorbed by boreal conifer forests. *IEEE Transactions on Geoscience and Remote Sensing*, *34*, 1353−1368.

Conolly, J., Roulet, N. T., Seaquist, J. W., Holden, N. M., Lafleur, P. M., Humphreys, E. R., et al. (2009). Using MODIS derived *f*PAR with ground based flux tower measurements to derive the light use efficiency for two Canadian peatlands. *Biogeosciences*, *6*, 225−234.

Falge, E., Baldocchi, D., Olson, R., Anthoni, P., Aubinet, M., Bernhofer, C., et al. (2001). Gap filling strategies for defensible annual sums of net ecosystem exchange. *Agricultural and Forest Meteorology*, *107*, 43−69.

Fensholt, R., Sandholt, I., & Rasmussen, M. S. (2004). Evaluation of MODIS LAI, fAPAR and the relation between fAPAR and NDVI in a semi-arid environment using in situ measurements. *Remote Sensing of Environment*, *91*, 490−507.

Gao, F., Masek, J., Schwaller, M., & Hall, H. (2006). On the blending of the Landsat and MODIS surface reflectance: Predicting daily Landsat surface reflectance. *IEEE Transactions on Geosciences and Remote Sensing*, *44*, 2207−2218.

Gorham, E. (1991). Northern peatlands: Role in the carbon cycle and probable responses to climatic warming. *Ecological Applications*, *1*, 182−195.

Goward, S. N., & Huemmrich, K. F. (1992). Vegetation canopy PAR absorptance and the Normalized Difference Vegetation Index: An assessment using the SAIL model. *Remote Sensing of Environment*, *39*, 119−140.

Hall, F. G., Shimabukuro, Y. E., & Huemmrich, K. F. (1995). Remote sensing of forest biophysical structure mixture and decomposition using mixture decomposition and geometric reflectance models. *Ecological Applications*, *5*, 993−1013.

Heinsch, F. A., Reeves, M. C., Votava, P., Kang, S., Milesi, M., Zhao, C., et al. (2003). *User's guide — GPP and NPP (MOD17A2/A3) products — NASA MODIS land algorithm* (pp. 1−57). Missoula, MT: Univ. Montana.

Heinsch, F. A., Zhao, M., Running, S. W., Kimball, J. S., Nemani, R. R., Davis, K. J., et al. (2006). Evaluation of remote sensing based terrestrial productivity from MODIS using regional tower eddy flux network observations. *IEEE Transactions on Geosciences and Remote Sensing*, *44*, 1908−1925.

Hird, J. N., & McDermid, G. J. (2009). Noise reduction of NDVI time series: An empirical comparison of selected techniques. *Remote Sensing of Environment*, *113*, 248−258.

Huete, A., Didan, K., Miura, T., Rodriguez, E. P., Gao, X., & Ferreira, L. G. (2002). Overview of the radiometric and biophysical performance of the MODIS vegetation indices. *Remote Sensing of Environment*, *83*, 195−213.

Humphreys, E. R., Lafleur, P. M., Flanagan, L. B., Hedstrom, N., Syed, K. H., Glenn, A. J., et al. (2006). Summer carbon dioxide and water vapor fluxes across a range of northern peatlands. *Journal of Geophysical Research*, *111*, G04011. doi:10.1029/2005JG000111

Johansson, T., Malmer, N., Crill, P. M., Friborg, T., Åkerman, J., Mastepanov, M., et al. (2006). Decadal vegetation changes in a northern peatland, greenhouse gas fluxes and net radiative forcing. *Global Change Biology*, *12*, 2352−2369.

Jönsson, P., & Eklundh, L. (2002). Seasonality extraction by function fitting to time-series of satellite sensor data. *IEEE Transactions on Geoscience and Remote Sensing*, *40*, 1824−1832.

Jönsson, P., & Eklundh, L. (2004). TIMESAT — A program for analyzing time-series of satellite sensor data. *Computers and Geosciences*, *30*, 833−845.

Keeling, R. F., Piper, S. C., & Heimann, M. (1996). Global and hemispheric CO_2 sinks deduced from changes in atmospheric O_2 concentration. *Nature*, *381*, 218−221.

Krankina, O. N., Pflugmacher, D., Friedl, M., Cohen, W. B., Nelson, P., & Baccini, A. (2008). Meeting the challenge of mapping peatlands with remotely sensed data. *Biogeosciences*, *5*, 1809−1820.

Lafleur, P. M., Roulet, N. T., Bubier, J. L., Frolking, S., & Moore, T. R. (2003). Interannual variability in the peatland-atmosphere carbon dioxide exchange at an ombrotrophic bog. *Global Biogeochemical Cycles*, *17*, 1036. doi:10.1029/2002GB001983

Lagergren, F., Eklundh, L., Grelle, A., Lundblad, M., Mölder, M., Lankreijer, H., et al. (2005). Net primary production and light use efficiency in a mixed coniferous forest in Sweden. *Plant, Cell and Environment*, *28*, 412−423.

Lagergren, F., Grelle, A., Lankreijer, H., Mölder, M., & Lindroth, A. (2006). Current carbon balance of the forested area in Sweden and its sensitivity to global change as simulated by Biome-BGC. *Ecosystems*, *9*, 894−908.

Landelius, T., Josefsson, W., & Carlund, T. (2003). Operational mesoscale modelling of PAR, UV and global radiation. In J. R. Slusser, J. R. Herman, & W. Gao (Eds.), *Ultraviolet ground- and space-based measurements, models, and effects III*, *Vol. 5156*, Bellingham: Proceedings of SPIE.

Lindroth, A., Grelle, A., & Morén, A. -S. (1998). Long-term measurements of boreal forest carbon balance reveal large temperature sensitivity. *Global Change Biology*, *4*, 443−450.

Lindroth, A., Lund, M., Nilsson, M., Aurela, M., Christensen, T. R., Laurila, T., et al. (2007). Environmental controls on the CO_2 exchange in North European mires. *Tellus*, *59*, 812−825.

Lindroth, A., Lagergren, F., Aurela, M., Bjarnadottir, B., Christensen, T., Dellwik, E., et al. (2008). Leaf area index is the principal scaling parameter for both gross photosynthesis and ecosystem respiration of Northern deciduous and coniferous forests. *Tellus*, *60*, 129−142.

Lloyd, J., & Taylor, J. A. (1994). On the temperature dependence of soil respiration. *Functional Ecology*, *8*, 315−323.

Lund, M., Lindroth, A., Christensen, T. R., & Ström, L. (2007). Annual CO_2 balance of a temperate bog. *Tellus B*, *59*, 804−811.

Lund, M., Lafleur, P.M., Roulet, N.T., Lindroth, A., Christensen, T. R., Aurela, M., Chojnicki, B.H., Flanagan, L.B., Humphreys, E.R., Laurila, T., Oechel, W.C., Olejnik, J., Rinne, J., Schubert, P., & Nilsson, M.B. (2009a). Variability in exchange of CO2 across twelve northern peatland and tundra sites. Global Change Biology. (accepted)

Lund, M., Lindroth, A., Mastepanov, M., Ström, L., & Christensen, T. R. (2009b). Contemporary exchange of CO_2 and CH_4 in a temperate ombrotrophic bog. In M. Lund, *Peatlands at a threshold — greenhouse gas dynamics in a changing climate*. Lund, Sweden: Dissertation at the Department of Physical Geography and Ecosystems Analysis at Lund University.

Monteith, J. L. (1972). Solar radiation and productivity in tropical ecosystems. *Journal of Applied Ecology*, *9*, 747−766.

Monteith, J. L. (1977). Climate and the efficiency of crop production in Britain. *Philosophical Transactions of the Royal Society of London Series B: Biological Sciences*, *281*, 277−294.

Myneni, R. B., & Williams, D. L. (1994). On the relationship between FAPAR and NDVI. *Remote Sensing of Environment*, *49*, 200−211.

Nilsson, M., Sagerfors, J., Buffam, I., Laudon, H., Eriksson, T., Grelle, A., et al. (2008). Contemporary carbon accumulation in a boreal oligotrophic minerogenic mire — A significant sink after accounting for all C-fluxes. *Global Change Biology*, *14*, 2317−2332.

Olofsson, P., & Eklundh, L. (2007). Estimation of absorbed PAR across Scandinavia from satellite measurements. *Part II: Modeling and evaluating the fractional absorption. Remote Sensing of Environment*, *110*, 240−251.

Olofsson, P., Eklundh, L., Lagergren, L., Jönsson, P., & Lindroth, A. (2007). Estimating net primary production for Scandinavian forests using data from Terra/MODIS. *Advances in Space Research*, *39*, 125−130.

Olofsson, P., Lagergren, F., Lindroth, A., Lindström, J., Klemedtsson, L., Kutsch, W., et al. (2008). Towards operational remote sensing of forest carbon balance across Northern Europe. *Biogeosciences*, *5*, 817−832.

Prentice, I. C., Farquhar, G. D., Fasham, M. J. R., Goulden, M. L., Heimann, M., Jaramillo, V. J., Kheshgi, H. S., Le Quéré, C., Scholes, R. J., & Wallace, D. W. R. (2001). The carbon cycle and atmospheric carbon dioxide. In L. Pitelka & Ramirez Rojas, A. (Eds.), *Climate change 2001: The scientific basis. Contribution to the third assessment report of the Intergovernmental Panel on Climate Change* (pp. 185–237). Cambridge: Cambridge University Press.

Prince, S. D. (1991). A model of regional primary production for use with coarse resolution satellite data. *International Journal of Remote Sensing*, *6*, 1313−1330.

Rahman, A. F., Sims, D. A., Cordova, V. D., & El-Masri, B. Z. (2005). Potential of MODIS EVI and surface temperature for directly estimating per-pixel ecosystem C fluxes. *Geophysical Research Letters*, *32*, L19404. doi:10.1029/2005GL024127

Reichstein, M., Falge, E., Baldocchi, D., Papale, D., Aubinet, M., Berbigier, P., et al. (2005). On the separation of net ecosystem exchange into assimilation and ecosystem respiration: Review and improved algorithm. *Global Change Biology*, *11*, 1424−1439.

Riutta, T., Laine, J., Aurela, M., Rinne, J., Vesala, T., Laurila, T., et al. (2007). Spatial variation in plant community functions regulates carbon gas dynamics in a boreal fen ecosystem. *Tellus B*, *59*, 838−852.

Roulet, N. T., Lafleur, P. M., Richard, P. J. H., Moore, T. R., Humphreys, E. R., & Bubier, J. (2007). Contemporary carbon balance and late Holocene carbon accumulation in a northern peatland. *Global Change Biology*, *13*, 397−411.

Rouse, J. W., Haas, R. H., Schell, J. A., & Deering, D. W. (1973). Monitoring vegetation systems in the Great Plains with ERTS. *Third ERTS Symposium, NASA SP-351 I* (pp. 309−317).

Ruimy, A., Saugier, B., & Dedieu, G. (1994). Methodology for the estimation of terrestrial net primary production from remotely sensed data. *Journal of Geophysical Research*, *99*, 5263−5283.

Running, S. W., Nemani, R. R., Heinsch, F. A., Zhao, M., Reeves, M., & Hashimoto, H. (2004). A continuous satellite-derived measure of global terrestrial primary production. *Bioscience*, *54*, 547−560.

Rydin, H., & Jeglum, J. (2006). The biology of peatlands. New York: Oxford University Press Glossary.

Sagerfors, J., Lindroth, A., Grelle, A., Klemedtsson, L., Weslien, P., & Nilsson, M. (2008). Annual CO_2 exchange between a nutrient-poor, minerotrophic, boreal mire and the atmosphere. *Journal of Geophysical Research*, *113*, G01001. doi:10.1029/2006JG000306

Sims, D. A., Rahman, A. F., Cordova, V. D., El-Masri, B. Z., Baldocchi, D. D., Flanagan, L. B., et al. (2006). On the use of MODIS EVI to assess gross primary productivity of North American ecosystems. *Journal of Geophysical Research*, *111*, G04015. doi:10.1029/2006JG000162

Sims, D. A., Rahman, A. F., Cordova, V. D., El-Masri, B. Z., Baldocchi, D. D., Bolstad, P. V., et al. (2008). A new model of gross primary productivity for North American ecosystems based solely on the enhanced vegetation index and land surface temperature from MODIS. *Remote Sensing of Environment*, *112*, 1633—1646.

Tan, B., Woodcock, C. E., Hu, J., Zhang, P., Ozdogan, M., Huang, D., et al. (2006). The impact of gridding artifacts on the local spatial properties of MODIS data: Implications for validation, compositing, and band-to-band registration across resolutions. *Remote Sensing of Environment*, *105*, 98—114.

Tarnocai, C. (2006). The effect of climate change on carbon in Canadian peatlands. *Global and Planetary Change*, *53*, 222—232.

Tucker, C. J., Fung, I. Y., Keeling, C. D., & Gammon, R. H. (1986). The relationship of global green leaf biomass to atmospheric CO_2 concentrations. *Nature*, *319*, 159—199.

Turner, D. P., Gower, S. T., Cohen, W. B., Gregory, M., & Maiersperger, T. K. (2002). Effects of spatial variability in light use efficiency on satellite based NPP monitoring. *Remote Sensing of Environment*, *80*, 397—405.

Turner, D. P., Ritts, W. D., Cohen, W. B., Maiersperger, T. K., Gower, S. T., Kirschbaum, A. A., et al. (2005). Site-level evaluation of satellite-based global terrestrial gross primary production and net primary production monitoring. *Global Change Biology*, *11*, 666—684.

Turunen, J., Tomppo, E., Tolonen, K., & Reinikainen, A. (2002). Estimating carbon accumulation rates of undrained mires in Finland — Application to boreal and subarctic regions. *Holocene*, *12*, 69—80.

Vogelmann, J. E., & Moss, D. M. (1993). Spectral reflectance measurements in the genus *Sphagnum*. *Remote Sensing of Environment*, *45*, 273—279.

Wofsy, S. C., Goulden, M. L., Munger, J. W., Fan, S. M., Bakwin, P. S., Daube, B. C., et al. (1993). Net exchange of CO_2 in a mid-latitude forest. *Science*, *260*, 1314—1317.